Perpendicularly magnetized Mn-Co-Ga-based thin films with high coercive field.

Siham Ouardi,[1] Takahide Kubota,[2] Gerhard H. Fecher,[1] Rolf Stinshoff,[1] Shigemi Mizukami,[2] Terunobu Miyazaki,[2] Eiji Ikenaga,[3] and Claudia Felser[1, a)]

[1)] *Max Planck Institute for Chemical Physics of Solids, 01187 Dresden, Germany.*

[2)] *WPI-Advanced Institute for Materials Research (WPI-AIMR), Tohoku University, Sendai 980-8577, Japan*

[3)] *Japan Synchrotron Radiation Research Institute, SPring-8, Hyogo 679-5198, Japan*

(Dated: 13 November 2012)

$Mn_{3-x}Co_xGa$ epitaxial thin films were grown on MgO substrates by magnetron co-sputtering. Structures were tetragonal or cubic depending on Co content. Composition dependence of saturation magnetization and uniaxial magnetic anisotropy K_u of the films were investigated. A high K_u (1.2 MJ m^{-3}) was achieved for the $Mn_{2.6}Co_{0.3}Ga_{1.1}$ film with the magnetic moment $0.84\mu_B$. Valence band spectra were obtained by hard X-ray photoelectron spectroscopy. Sharp peaks in the cubic case, which were absent in the tetragonal case, prove that a *van Hove* singularity causes a *band Jahn–Teller effect* with tetragonal distortion. Observations agree well with the first–principles calculations.

[a)]Electronic mail: felser@cpfs.mpg.de

The tetragonally distorted Heusler compound Mn_3Ga with a DO_{22} structure has attracted considerable attention as a potential candidate for spin-transfer torque (STT) applications. Mn_3Ga has been proposed for use in STT applications as a compensated ferrimagnet exhibiting half-metallicity with 88% polarization, high Curie temperature T_c (730 K), and hard magnetic properties [1,2]. The epitaxial growth of Mn-Ga thin films with giant perpendicular magnetic anisotropy (PMA)[3–6] and high tunnel magnetoresistance (TMR)[7,8] have been successfully realized. According to the Slonczewski - Berger equation[9,10], in order to optimize materials for STT application (such as minimization of the switching current), the saturation magnetization M_s and Gilbert damping have to be minimized. The use of off-stoichiometric Mn_3Ga with Mn deficit demonstrates the possibility of increasing the magnetic energy products of the material; however, M_s also correspondingly increases[2].

Recently, it has been shown that partial substitution of Mn by Co in $Mn_{3-x}Co_xGa$ leads to a reduced saturation magnetization M_s[11,12]. The system exhibits a tetragonal structure for Co concentrations lower than $x = 0.4$. Similar to Mn_3Ga, it crystallizes in a tetragonally distorted variation of the Heusler structure and exhibits comparably hard ferrimagnetic properties. On the other hand, Co-rich alloys ($x > 0.5$) crystallize as cubic and magnetically soft structures. The tetragonal distortion of the cubic Heusler structure is caused by electronic instabilities corresponding to a band–type Jahn-Teller effect[13]. However, in contrast to the $Mn_{3-x}Rh_xSn$ system, the Curie temperature is still high[12]. Magnetic circular dichroism in X-ray absorption (XMCD) has been used to confirm the ferrimagnetic character of the $Mn_{3-x}Co_xGa$ system, with Mn atoms occupying two different sublattices with antiparallel spin orientation and different degrees of spin localization[14]. Ferrimagnetic characteristics were also similarly confirmed for epitaxial cubic thin films of Mn_2CoGa[15]. To identify the existence of a high density of states (DOS) at the Fermi energy (*van Hove* singularity) in such films, a convenient experiment such as photoelecton spectroscopy is required to be performed.

In the present study, epitaxial thin films of $Mn_{3-x}Co_xGa$ with varying levels of Co content were grown directly on MgO substrates. The electronic structure of the films was determined by all-electron *ab initio* calculations. The valence states of the films close to the Fermi energy were investigated by means of hard X-ray photoelectron spectroscopy, and the obtained results were compared with the calculations. The magnetic properties of the films were investigated and compared with those of the corresponding bulk material.

Epitaxial 30-nm thin films with nominal compositions of $Mn_{2.6}Co_{0.3}Ga_{1.1}$ and $Mn_{2.1}CoGa_{0.9}$ were grown on a MgO (001) single crystalline substrate using an ultrahigh-vacuum magnetron sputtering system. A Mn-Ga target and an elemental Co target were used for the deposition. Structural analysis was performed by means of out-of-plane and in-plane X-ray diffractometers (XRD). The magnetic properties of the films were investigated using a vibrating sample magnetometer (VSM) with a maximum applied field of 2 T at room temperature.

The valence band spectra of the films were measured by hard X-ray photoelectron spectroscopy (HAXPES) using the undulator beamline BL47XU at SPring-8 (Japan). Details of the HAXPES experiment have been previously reported[16–18]. For comparison, we use the electronic structure calculations performed by means of the fully relativistic spin–polarized KKR (Korringa–Kohn–Rostoker) method including a coherent potential approximation to account for random site occupation[19].

Figure 1 shows the XRD 2θ-ω pattern of $Mn_{2.6}Co_{0.3}Ga_{1.1}$ film. In addition to the peaks originating due to MgO, only the (002) and (004) peacks can be observed, thereby indicating that the $Mn_{2.6}Co_{0.3}Ga_{1.1}$ film is grown with the tetragonal c axis, wish is along the normal direction. The lattice constants are $a = 3.94$ Å and $c = 6.85$ Å. Furthermore, azimuthal (φ) scans were employed to confirm the crystalline structure of the film. The presence of (011) reflex in the film–as shown in the inset of Figure 1–indicates crystallization in a tetragonal $D0_{22}$-type structure[3]. The $Mn_{2.1}CoGa_{0.9}$ film shows a cubic structure with a lattice constant of $a = 5.889$ Å.

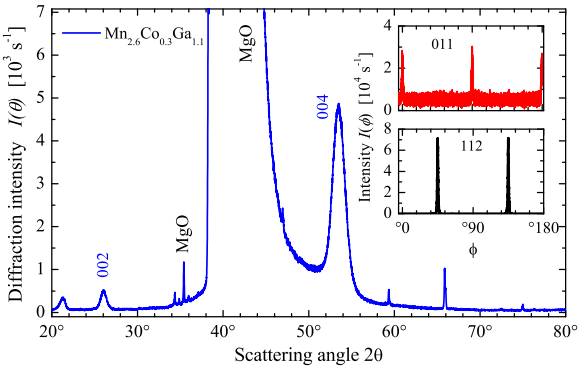

FIG. 1. X-ray diffraction pattern for 30-nm-thick $Mn_{2.6}Co_{0.3}Ga_{1.1}$ film. The insets show the azimuthal scans of the (011) (top) and (112) (bottom) planes.

Figures 2(a) and 2(b) show the hysteresis loops of the $Mn_{2.6}Co_{0.3}Ga$ and $Mn_{2.1}CoGa_{0.9}$ films, respectively. The magnetic field was applied perpendicular ($\perp$) or in-plane ($\parallel$) to the film plane direction. When a magnetic field is applied perpendicular to the film plane, the magnetization curves of the film with less Co content ($Mn_{2.6}Co_{0.3}Ga$) exhibit a rectangular shape, whereas those of $Mn_{2.1}CoGa_{0.9}$ exhibit a soft magnetic behavior.

It is significant that the coercitive field H_c of the $Mn_{2.6}Co_{0.3}Ga$ film is large when compared with the corresponding values reported previously[6]. The results indicate that the easy axis of the magnetization is perpendicular to the film plane in the tetragonal case. For comparison, the hysteresis of polycrystalline $Mn_{2.6}Co_{0.3}Ga$ bulk material was measured; the results are shown in Fig. 2(a). The coercive field is obviously smaller compared with that of the thin film. The bulk sample is not saturated even at fields of $\mu_0 H = 6$ T (outside the range shown in the figure). However, the magnetic moments per formula unit are of the same order as those of the films. This non–saturating behavior is typical for polycrystalline samples consisting of randomly oriented grains with different alignment of the easy or hard magnetization directions.

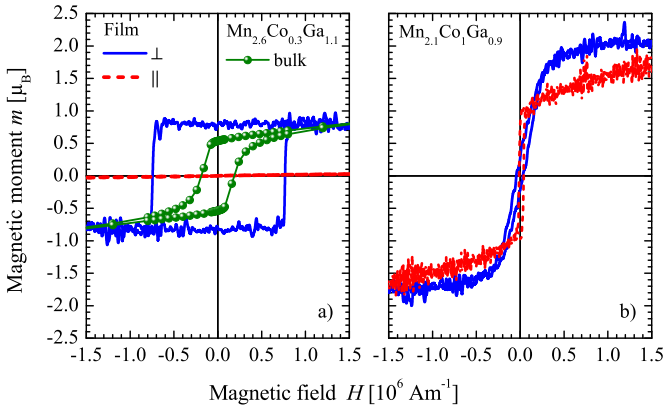

FIG. 2. Perpendicular($\perp$) and in–plan($\parallel$) hysteresis curves of (a) tetragonal $Mn_{2.6}Co_{0.3}Ga_{1.1}$ and (b) cubic $Mn_{2.1}Co_1Ga_{0.9}$ thin films.

The uniaxial anisotropy constant K_u was estimated using the relation as described in a previous work[6]. The effective anisotropy field H_{eff} was obtained by the extrapolated intersection of the in–plane $M - H$ curve with the saturation magnetization value of the perpendicular $M-H$ curve. The magnetic moment m, uniaxial magnetic anisotropy K_u, and coercive field H_c of the films are compared in Table I. The Co–doped film $Mn_{2.6}Co_{0.3}Ga_{1.1}$

shows a high uniaxial magnetic anisotropy K_u as previously reported magnetic anisotropy values for Mn-Ga films. Further, the film exhibits a high coercive field of 7.74×10^5 A m^{-1} and remanence of 0.33 T. These values are comparably higher than those obtained for polycrystalline bulk materials. The cubic $Mn_{2.1}CoGa_{0.9}$ shows a soft magnetic behavior, as reported for half metallic Heusler compounds[11].

TABLE I. Composition dependence of magnetic moment m (per formula unit), uniaxial magnetic anisotropy K_u, coercive field H_c, remanence B_r, specific maximum energy product $(BH)_{max}$, and specific energy integral W_h of different $Mn_{3-x}Co_xGa$ films compared with bulk materials. The bulk $Mn_{2.6}Co_{0.3}Ga_{1.1}$ was not saturated.

	m	K_u	H_c	B_r	$(BH)_{max}$
	μ_B	M J m^{-3}	k A m^{-1}	T	k J m^{-3}
$Mn_{2.1}CoGa_{0.9}$ (cubic)	2.03	-	24	0.08	0.38
$Mn_{2.6}Co_{0.3}Ga_{1.1}$	0.84	1.2	757	0.33	24
Mn_3Ga [Ref.[6]]	-	1.0 - 1.5	-	-	-
Mn_3Ga [Ref.[4]]	-	0.89	-	-	
$Mn_{2.6}Co_{0.3}Ga_{1.1}$ bulk	n.s.	-	199	0.12	2.61
Mn_3Ga bulk [Ref.[1,2]]	1.0	-	453	0.136	18.3

The magnetic materials are also characterized by various magnetic energies besides anisotropy, coercive field, and remanence[20]. An important energy parameter of interest is the maximum energy product $BH_{max} = \max(-B \times H)$. It represents the maximum useful magnetic energy of a permanent magnet. Its value is obtained by multiplying B times H in the second (or fourth) quadrant of the hysteresis loop. The specific energy integral $W_H = \oint H dB$ is from direct integration of the magnetization loops and the hysteresis loss per cycle. For an ideal hard magnet, a nearly rectangular hysteresis loop ($B(H)$) with $W_H \approx 4 \times BH_{max}$ is expected. Magnetic energies of the different samples are compared in Table I together with the other magnetic data.

The electronic structures of $Mn_{2.6}Co_{0.3}Ga_{1.1}$ and $Mn_{2.1}Co_1Ga_{0.9}$ were investigated using HAXPES at room temperature. Figure 3 compares the measured valence band spectra to the calculated total density of states (DOS). All the major structures observed in the spectra are in good agreement with the calculated DOS. The intensity ratios of the peaks

are different from the calculated DOS. This deviation arises from the different partial cross sections of the s, p, and d states that are localized at different atoms of the material[21].

The low–lying maximum at about -8 eV below the Fermi edge ϵ_F arises from the a_1 (s) states being localized at the Ga atoms. These states are broader for $Mn_{2.6}Co_{0.3}Ga_{1.1}$ with an additional shoulder being present at about -6.7 eV. Such states arise due to the presence of the additional Ga atoms, which are located at the 2b Wyckoff position that is normally occupied by Mn.

An interesting feature here is the significant changes observed in the spectra close to ϵ_F, as shown in Figure 3(c), where the spectral values indicate the difference between the tetragonal $Mn_{2.6}Co_{0.3}Ga_{1.1}$ and the cubic $Mn_{2.1}CoGa_{0.9}$ films. In the cubic case, a sharp peak at -0.94 eV is evident, whereas for the tetragonal films, the corresponding states are smeared out. This change in the electronic structure is due to a *van Hove* singularity occurring close below the Fermi energy. Changing the composition of the compound shifts this van Hove singularity to the Fermi energy. This causes a *band Jahn-Teller effect* that results in the tetragonal distortion of the crystalline structure upon changing the number of valence electrons[12].

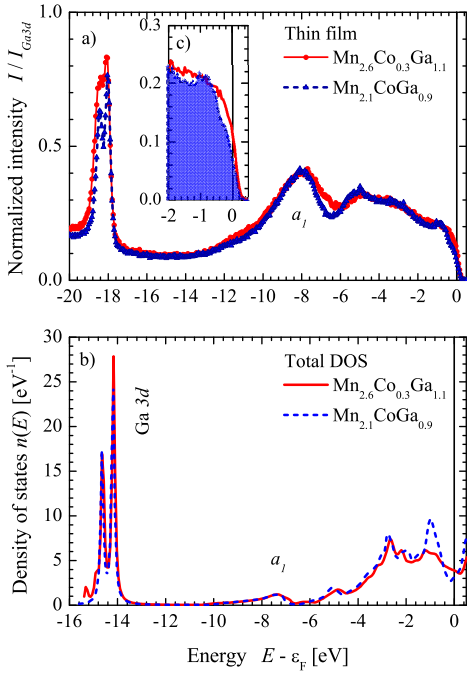

FIG. 3. (a) Valence band spectra and (b) total density of states of $Mn_{2.6}Co_{0.3}Ga_{1.1}$ and $Mn_{2.1}Co_1Ga_{0.9}$ films. (c) Region close to the Fermi energy ϵ_F on an enlarged scale.

An inspection of Figure 3 might lead to the assumption that the obtained data contradicts the above statement as both the DOS and the intensity at ϵ_F are seemingly higher in the tetragonal case. Here, it should be mentioned that the high density in the cubic case is still tot close to ϵ_F. Further, the molecular Jahn–Teller effect is not completely valid for solids. Instead of observing a bare splitting of the states at the Γ-point, we can observe changes in all energy bands that are coupled to each other. The energy gain by removing the van Hove singularity from the Fermi energy is given by the change in the band energy $E_{\mathrm{Band}} = \int_0^{\epsilon_F} E \cdot N(E) dE$ when the density of states $N(E)$ changes with the structure. The obtained result is different from the energy gain obtained by the simple splitting of a state.

In summary, epitaxial thin films of $Mn_{3-x}Co_xGa$ were grown with varying levels of Co content. Depending on the Co content level, tetragonal and cubic structures were is performed. The composition dependence of the saturation magnetization M_S and uniaxial magnetic anisotropy K_u in the epitaxial films were investigated. A high magnetic anisotropy K_u of 1.2 MJ m^{-3} was achieved for the tetragonal $Mn_{2.6}Co_{0.3}Ga_{1.1}$ film with a low magnetic moment m_S of $0.84\mu_B$.

Furthermore, the valence band of the films was examined by HAXPES to study the structural dependence of the electronic structure of the Co–doped Mn-Ga films. A van Hove singularity close to the Fermi edge is observed in the cubic films, whereas the corresponding energy states are smeared out in the tetragonal films due to the presence of the band Jahn-Teller distortion.

ACKNOWLEDGMENTS

The authors gratefully acknowledge financial support by the DfG-JST (P 1.3-A and 2.1-A in FOR 1464 ASPIMATT). The synchrotron–based HAXPES measurements were performed at the beamline BL47XU of SPring-8 facility with the approval of JASRI (Proposal No. 2012A0043).

REFERENCES

[1]B. Balke, H. G. Fecher, J. Winterlik, and C. Felser, App. Phys. Lett. **90**, 152504 (2007).

[2]J. Winterlik, B. Balke, G. H. Fecher, C. Felser, M. C. M. Alves, F. Bernardi, and J. Morais, Phys. Rev. B **77**, 054406 (2008).

[3]F. Wu, S. Mizukami, D. Watanabe, H. Naganuma, M. Oogane, Y. Ando, and T. Miyazaki, App. Phys. Lett. **94**, 122503 (2009).

[4]H. Kurt, K. Rode, M. Venkatesan, P. Stamenov, and J. M. D. Coey, Phys. Rev. B **83**, 020405 (2011).

[5]S. Mizukami, F. Wu, A. Sakuma, J. Walowski, D. Watanabe, T. Kubota, X. Zhang, H. Naganuma, M. Oogane, Y. Ando, and T. Miyazaki, Phys. Rev. Lett. **106**, 117201 (2011).

[6]S. Mizukami, T. Kubota, F. Wu, X. Zhang, T. Miyazaki, H. Naganuma, M. Oogane, A. Sakuma, and Y. Ando, Phys. Rev. B **85**, 014416 (2012).

[7]T. Kubota, M. Araidai, S. Mizukami, X. Zhang, Q. Ma, H. Naganuma, M. Oogane, Y. Ando, M. Tsukada, and T. Miyazaki, App. Phys. Lett. **99**, 192509 (2011).

[8]T. Kubota, Q. Ma, S. Mizukami, X. Zhang, Y. Miura, H. Naganuma, M. Oogane, Y. Ando, and T. Miyazaki, Appl. Phys. Express **5**, 043002 (2012).

[9]J. C. Slonczewski, J. Magn. Magn. Mater. **159**, L1 (1996).

[10]L. Berger, Phys. Rev. B **54**, 9353 (1996).

[11]V. Alijani, J. Winterlik, H. G. Fecher, and C. Felser, App. Phys. Lett. **99**, 222510 (2011).

[12]J. Winterlik, S. Chadov, A. Gupta, V. Alijani, T. Gasi, K. Filsinger, B. Balke, G. H. Fecher, C. A. Jenkins, F. Casper, J. Kübler, G.-D. Liu, L. Gao, S. S. P. Parkin, and C. Felser, Adv. Mater. (2012).

[13]S. Chadov, J. Kiss, and C. Felser, Adv. Funct. Mater. , doi: 10.1002/adfm.201201693 (2012).

[14]P. Klaer, C. A. Jenkins, V. Alijani, J. Winterlik, B. Balke, C. Felser, and H. J. Elmers, App. Phys. Lett. **98**, 212510 (2011).

[15]M. Meinert, J.-M. Schmalhorst, C. Klewe, G. Reiss, E. Arenholz, T. Böhnert, and K. Nielsch, Phys. Rev. B **84**, 132405 (2011).

[16]S. Ouardi, C. Shekhar, G. H. Fecher, X. Kozina, G. Stryganyuk, C. Felser, S. Ueda, and K. Kobayashi, Appl. Phys. Lett. **98**, 211901 (2011).

[17]S. Ouardi, G. H. Fecher, X. Kozina, G. Stryganyuk, B. Balke, C. Felser, E. Ikenaga, and K. Kobayashi, Phys. Rev. Lett. **107**, 036402 (2011).

[18]C. Shekhar, S. Ouardi, G. H. Fecher, A. K. Nayak, C. Felser, and E. Ikenaga, Appl. Phys.

Lett. **100**, 252109 (2012).

[19]H. Ebert, D. Ködderitzsch, and J. Minar, Rep. Prog. Phys **74**, 096501 (2011).

[20]J. M. D. Coey, *Magnetism and Magnetic Materials* (Cambridge University Press, Cambridge, 2010).

[21]G. H. Fecher, B. Balke, S. Ouardi, C. Felser, G. Schönhense, E. Ikenaga, J. J. Kim, S. Ueda, and K. Kobayashi, J. Phys. D: Appl. Phys. **40**, 1576 (2007).